www.papersinphysics.org

Received: 01 July 2025, Accepted: 24 December 2025
Edited by: Laura Foin, Université Paris-Saclay, France
Licence: Creative Commons Attribution 4.0
DOI: https://doi.org/10.4279/PIP.180003

ISSN 1852-4249

Exploring zinc oxide/cerium oxide/indium tin oxide nano-structures as LEDs: An optical and structural investigation

Zehraa Najim Abdul-ameer[1*]

Multilayer optoelectronic devices play a crucial role due to their ability to combine the novel properties of dissimilar materials for superior performance leading to enhanced or novel functionalities. This study focuses on designing, fabricating and characterizing a novel nano multilayer structure of zinc oxide/cerium oxide/ITO in a simple chemical method. X-ray diffraction (XRD) and scanning electron Microscopy (SEM), UV-visible, and photoluminescence were investigated. Optical properties revealed two wide band gaps of 3.15eV for prepared multilayer structures. The multilayer devices exhibit a broad photoluminescent peak at 340eV. Results show significant improvements in charge carrier, optical absorption and quantum efficiency. Addition of the cerium layer enhances conductivity and photocurrent of nano structures by facilitating electron-hole pair separation under photo excitation. These findings highlight the importance of the prepared multilayer nano structure in various optoelectronic technologies such as photodetectors, sensors and light emitting diodes.

I Introduction

Triple layer nanostructures play important roles in optoelectronics fabrication as they have transformative fields that take advantage of unique properties to achieve enhanced performance in optoelectronic devices. Optoelectronic devices are essential because they transform electrical signals into light and then back again, allowing communication, sensor and visual display technologies — such as LEDs, laser diodes and photodetectors — found in everything from fiber optics to cameras to light detectors [1, 2]. Cerium oxide, commonly known as ceria (CeO2) is a transparent conducting oxide (TCO) with a wide band gap ($\sim$ 3.2eV), and unique physical properties [3]. Its cubic structure and ability to switch oxidation states make it an important material for advancing technologies [4]. ZnO is another transparent conducting oxide with a large band gap ($\sim$ 3.3 eV) and hexagonal crystal structure, which exhibits exceptional optical [4], structural [5], and electronic properties. The addition of zinc oxide to cerium oxide offers several advantages due to their complementary properties. Both metal oxides have wide band gaps and their combination leads to enhancement in performance of optoelectronic devices [8].

The current research focuses on optimizing cerium properties by fabrication of multilayer nano structured zinc oxide/cerium oxide/indium tin oxide and characterizing its structural, optical, and electrical properties to investigate efficiency of heterostructures as light emitting diodes.

II Experimental details

The study employed (0.01) mol of cerium nitrate hexahydrate solution with a dilute ammonia solution. Cerium nitrate hex hydrate was dissolved in double deionized H_2O and precipitated by the drop wise addition of the obtained solution to the ammonia solution. Water-soluble species were then removed by deionized water washing. Ethanol was then used to remove water

* zehraa.najim@sc.uobaghdad.edu.iq

[1] Department of Remote Sensing and GIS, College of Science, University of Baghdad, Iraq.

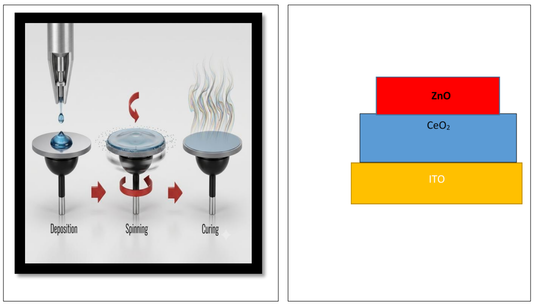

Figure 1: (a) spin coating technique (b) triple layer arrangement

and disrupt hydrogen bonded networks between water and the precursor. The obtained yellow precipitate was deposited on ITO and dried at 383 K for 12 h, and then calcined at 500 °C for 3 h [9].

Zinc nitrate hexahydrate was dissolved in deionized water under stirring, followed by slow addition of sodium hydroxide as (precipitating agent) until pH reached 10. A white precipitate of cerium oxide formed, then the solution was deposited, filtered, and washed several times with water and ethanol for impurities removal [10, 11]. Finally, the nano structure was dried at 100 °C then subject to calcination at 400-600°C [12].

2.3 Preparation of zinc oxide/cerium oxide/ITO triple layer was performed using spin coating (Fig. 1). The first layer structure of cerium dioxide solution was deposited on ITO substrate using spin coating technique, then filtered, washed and calcined at 600 °C

The second layer was zinc oxide solvent solution, deposited on the cerium oxide/ITO and spin coated, deposited, and calcined at 600 °C. The triple layer thickness of each layer, tested using the spectroscopic reflectometer Interferometer method, was used to determine the thickness for each layer using laser beam reflection of the He-Ne laser (632.8 nm) [13]:

$$d = \frac{\Delta s}{s} \cdot \frac{\lambda}{2}. \qquad (1)$$

As d is thickness in nm, Δs is fringe distance, and s is fringe width, the thickness of each layer was approximately 150 nm.

III Results and discussion

Morphology of the multilayer was investigated using X-ray diffraction with Cu-Kα radiation of ($\lambda = 1.54056$ Å), with Cerium oxide patterns at $2\theta = 28.5$, 33, 47.5, 56.5, 59.5, 69.5, 76.5, 79.5° corresponding to (111), (200), (220), (331), (220), (400), (331), (420), (422) (JPCD-34-0394), as in Fig. 2. ZnO patterns are 2θ =31.1, 32.97, 34.25, 43.31, 52.21, 52.81, 60.11, 66.83° corresponding to (100), (002), (110), (103) (200); the crystallite size was calculated using the Scherer equation. Crystallite size is as below [13]:

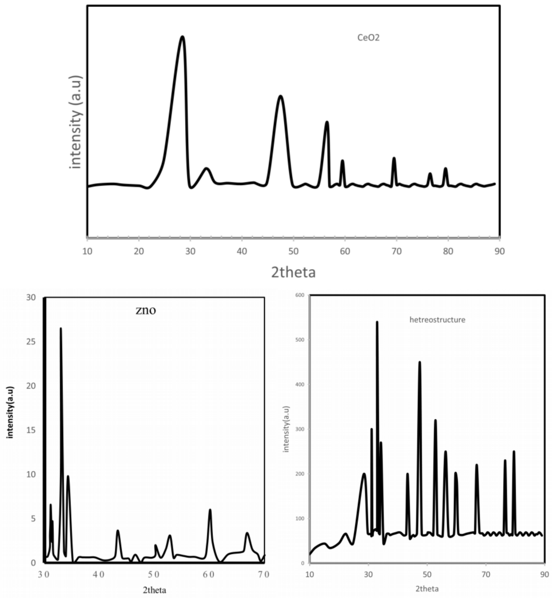

Figure 2: XRD patterns for ZnO, CeO_2, ZnO/CeO_2, and hetereostucture

$$d = \frac{\Delta s}{s} \cdot \frac{\lambda}{2}. \qquad (2)$$

The micro-strain (ϵ) was determined using equation [14]:

$$\epsilon = \frac{\beta \cos\theta}{4}, \qquad (3)$$

where ϵ is the average micro-strain of the heterostructure which represents disarrangement of lattice and the number of dislocations per unit area (dislocation density) as given in equation [15]:

$$\delta = \frac{1}{G^2}. \qquad (4)$$

Experimental results and calculations were used to calculate the XRD parameters as shown in Table (1):

Table 1: XRD parameters

Parameter	Zinc oxide	Cerium Dioxide	Heterostructure
(hkl)	(100), (002), (110), (103), (200)	(111), (200), (220), (331), (220), (400), (331), (420), (422)	(100), (002), (110), (103), (200), (111), (200), (220), (331), (220), (400), (331), (420), (422)
β (rad)	0.05	0.018	0.02
G (nm)	18.5	69.3	33.5
ε (10^{-3}lines^{-2}.m^{-4})	683	765	452
δ (1/nm^2)	2.9	2.1	2.3

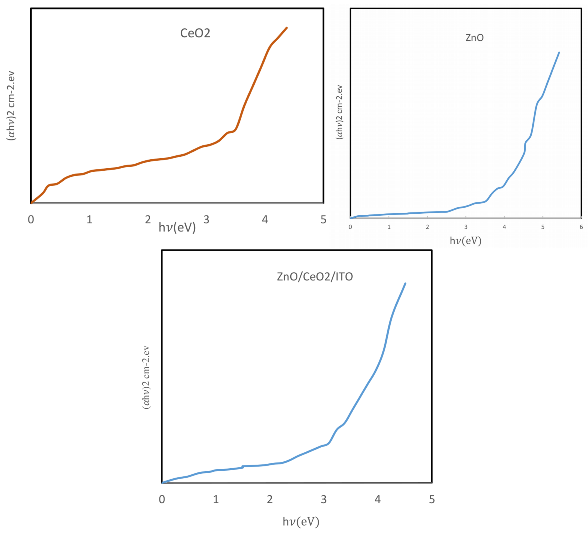

Figure 3: Band gap for samples

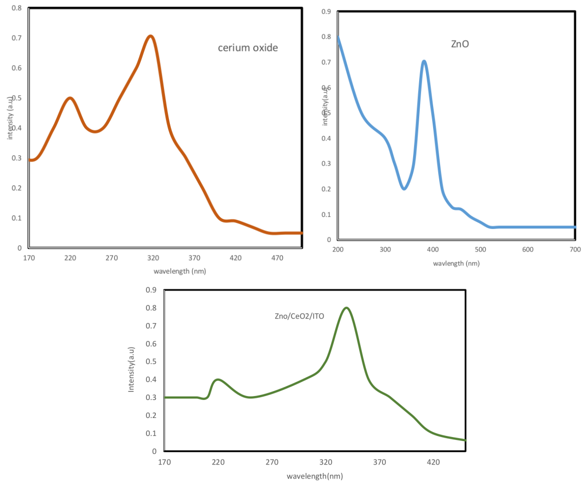

Figure 4: Photoluminescence for samples

i Optical properties

A UV-spectrophotometer-(Shimadzu) instrument is used to investigate optical properties so as to calculate the energy gap by Tauc equation [16]:

$$(\alpha h\nu)^2 = A(h\nu - E_g)^n \tag{5}$$

where hν is the energy of the photon, E_g is the band gap energy, and α is the coefficient of absorption.

From Fig. 3, cerium oxide shows 3.3 eV in comparison with bulk cerium oxide (3.0-3.3 eV). As particle size decreases, band gap increases due to spatial confinement of charge carriers. Cerium oxide exhibits transition from p-orbital to 5d orbital, which, located in the UV-range, reflects oxygen vacancies from state defects through the band gap [17].

Figure 3 shows a large band gap for ZnO (3.2 eV) due to Zn^+ interstitials which reduce donor states and oxygen vacancies that create trap states within the band gap, in comparison with bulk, which refers to the confinement effect[18]. The heterostructure shows improvement in the energy band gap with reference to the addition of a zinc oxide layer to cerium oxide, the heterostructure band gap was found to be (3.0 eV), representing an improvement in optical properties and marking this heterostructure as a candidate for various applications.

Photoluminescence emission, Fig. 4, depends on the energy difference between the defect state and valence band. For ceria, the PL shows visible luminescence in the UV- region that may refer to interstitial defects around 320 nm. So, the presence of Ce^{+3} ions near vacancies influences emission wavelength. For ZnO

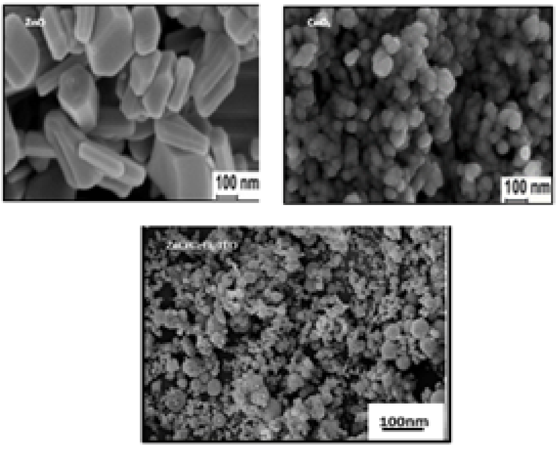

Figure 5: SEM images for ZnO, CeO_2, ZnO/CeO_2/ITO

nano particles, exciton absorption is found to be 380 nm; for CeO2 nano particles exciton absorption is found to be 364 nm. The multilayer nano structure exhibits near the visible region about 340 nm; when photons of greater energy pass across the semiconductor energy gap, an electron is moved from the valence band to the conduction band causing an anticipated increase in the material absorbency to the wavelength when compared to the band gap energy [18]. Scanning electron microscope images for ZnO nanoparticles shows nanorod shapes with particle sizes of about 10nm, and bodies with hexagonal bases with irregularly oriented aggregates.

Perpendicular to the substrate with average diameters of about 60nm, according to growth conditions, these nano rods can be ideal for many applications [19]. The spherical shape of cerium oxide, with some agglomerations, and particle sizes of about 15nm, with a rough texture, makes it a candidate for many applications such as optoelectronics and sensors, as shown in Fig. 5[20].

ii Electrical properties

Electrical properties are essential in investigating efficiency of light emiting diodes, these properties including Hall Effect RH, carrier concentration N, mobility μ, and conductivity of layer calculated from equation [21]:

$$\sigma = L/RA, \quad (6)$$

where L is the distance between electrodes, A is area, R (resistance in ohm). The Hall coefficient is calculated

Figure 6: I-V characteristic test system

from equation [21]:

$$R_H = 1/Ne. \quad (7)$$

The synthesized heterostructure shows high mobility and carrier concentration which enhance LED efficiency, facilitating electron - hole recombination and leading to increased light emission, as shown in Table 2. Voltage-current characterization was tested across the heterostructure, as shown in Fig. 6. When a voltage source is connected to both ends of the P-N junction, the holes, which are the majority charge carriers in the P layer, will move away from the positive terminal, and the free electrons, which are the majority charge carriers, will move away from the negative terminal of the source.

The majority charge carriers (holes and free electrons) will move towards the barrier, and if a voltage (V) greater than the barrier voltage is applied, this means that the electrons will cross the barrier as a result of overcoming the barrier voltage, resulting in the passage of an electric current whose value depends on the value of the junction voltage, as in Fig. 7.

I-V generates two regions, the first representing the current of recombination, the second representing tun-

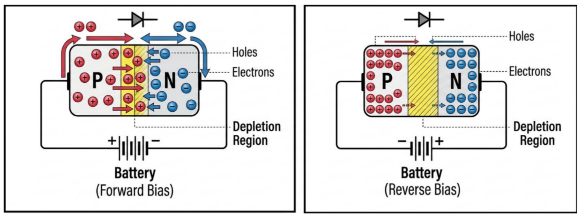

Figure 7: Forward and reverse bias

Table 2: Electrical parameters

Parameter	**ZnO**	**CeO_2**	**ZnO/CeO_2**
Carrier concentration (cm^{-3})	10^{16}	10^{12}	10^{20}
Mobility (cm^2/V·s)	5	7	26
Hall effect (cm^3/C)	0.6	0.5	0.3
Activation energy (eV)	0.4	0.54	0.78
Conductivity $(\Omega\cdot cm)^{-1}$	6.4×10^{-6}	0.0026×10^{-6}	0.93×10^{-6}

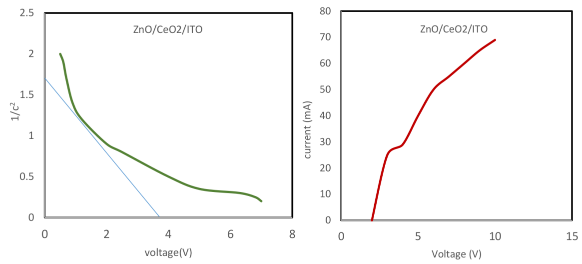

Figure 8: Electrical properties

neling current. The forward current arises throughout the heterostructure under illumination, which is a good sign for optoelectronic devices such as solar cells, sensors and LEDs. In the dark, the current is weak so it may make this heterostructure a candidate for photodiode applications.

IV Conclusion

This study demonstrates the ZnO/CeO_2/ITO heterostructure, which exhibits promising structural, optical, and electrical properties for optoelectronic applications such as photodetectors, sensors, and LEDs. This research explores the design, fabrication, and characterization of heterostructure ZnO/CeO_2/ITO. Advanced characterization techniques including X-ray diffraction (XRD), scanning electron microscopy (SEM), and photoluminsecence (PL) spectroscopy reveal improvement in structural and optoelectronic properties of the heterostructure. Electronic properties show improvements in charge carrier separation, optical absorption, and quantum efficiency. The heterostructure exhibits efficient electron-hole pair separation under photo excitation. Furthermore, the incorporation of CeO_2 introduces oxygen vacancy defects, which enhance conductivity (Fig 8), critical for applications in photodetectors and light-emitting diodes (LEDs).

[1] P. V. Pham, S. C. Bodepudi, et al., *2D Heterostructures for Ubiquitous Electronics and Optoelectronics: Principles, Opportunities, and Challenges*, Chem. Rev., **122**, 6514 (2022).

[2] Z. Abdul-Ameer, *ZnO/CuO/CdS Heterojunction Nanostructures as N-P-N for Optoelectronic Applications Effectiveness of*, Iraqi J. Sci., **65**, 10 (2024).

[3] T. Montini, M. Melchionna, et al., *Fundamentals and Catalytic Applications of CeO2-Based Materials*, Chem. Rev., **116**, 5987 (2016).

[4] P. Reshma, K. Ashwini, *Cerium Oxide Nanoparticles: Synthesis, Characterization and Study of Antimicrobial Activity*, J. Nanomater., **6**, 1000219 (2017).

[5] Z. N. Abdul-Ameer, *Optimizing cuprous oxide thin films: enhancing structural and electrical properties*, Momento, **70**, 33 (2025).

[6] J. K. Jaiswal, S. M. Simon, *Potentials and pitfalls of fluorescent quantum dots for biological imaging*, Trends Cell Biol., **14**, 497 (2004).

[7] D. Yue et al., *Facile fabrication of MgZnO/ZnO composites for high performance thin film transistor*, J. Alloys Compd., **873**, 159840 (2021).

[8] Z. N. Abdul-Ameer, *Novelty Au Nanoparticles with Different Nano Sizes as an Acidity Sensor*, Rev. Compos. Mater. Av., **31**, 167 (2021).

[9] W.-X. Tang, P.-X. Gao, *Homogenization of nanowire-based composites with anisotropic unit-cell and layered substructure*, MRS Commun., **6**, 311 (2016).

[10] H. R. Ghorbani, F. P. Mehr, et al., *Synthesis of ZnO Nanoparticles by Precipitation Method*, Orient. J. Chem., **31**, 1219 (2015).

[11] S. Wirunchit, W. Koetniyom, *ZnO Nanoparticles Synthesis and Characterization by Hydrothermal Process for Biological Applications*, Phys. Status Solidi A, **220**, 2200364 (2022).

[12] Z. N. Abdul-Ameer, *Effective MgO/Alumina/ITO Nano Heterostructure as Smart Material for Light-Emitting Diode*, Momento, **67**, 67 (2023).

[13] R. H. Jabbar, I. H. Hilal, et al., *Comparison of the structural characteristics of Al and B company doped ZnO thin films dropped on Si pulsed by laser and porous silicon*, AIP Conf. Proc., **2611**, 030001 (2023).

[14] R. N. Jeyad, L. K. Abbas, *Optical And Structural Characteristics Of Sn-doped ZnS Thin Films For Sensing H2 Gas*, J. Opt., (2025).

[15] Z. N. Abdul-Ameer, *Studying the optical and nanostructural properties of CdS/NiO/ITO as a photodetector*, J. Opt., **53**, 5065 (2024).

[16] S. K. Mustafa, L. A. Abdullah, et al., *Study of the structural and optical properties of cadmium oxide prepared by the pulsed laser deposition method*, J. Opt., (2024).

[17] H. Kh. Al-Lamy, E. M. Nasir, et al., *Electrical properties of CdxSe1-x films at different thickness and annealing temperatures*, Dig. J. Nanomater. Biostruct., **15**, 143 (2020).

[18] Z. N. Abdul-Ameer, *A facile route for preparation of CdS nanoparticles*, Momento, **68**, 27 (2024).

[19] T. Masui, K. Fujiwara, et al., *Characterization of Cerium(IV) Oxide Ultrafine Particles Prepared Using Reversed Micelles*, Chem. Mater., **9**, 2197 (1997).

[20] J. J. Gulicovski, I. Bračko, et al., *Morphology and the isoelectric point of nanosized aqueous ceria sols*, Mater. Chem. Phys., **148**, 868 (2014).

[21] Z. N. Abdul-Ameer, *Synthesis and Characterization of CdS/CuAlO2/ITO Nano-heterostructures: A Novel LED for Optoelectronic Applications*, J. Opt., (2024).

[22] H. J. Jawad, A. F. Sultan, *Review Recent Developments In High-Power Diode Lasers For Biomedical Applications*, J. Opt., **54**, 763 (2024).